NANO LETTERS

2007
Vol. 7, No. 12
3650−3655

Synthesis of Platinum Nanowire Networks Using a Soft Template

Yujiang Song,*,† Robert M. Garcia,†,‡ Rachel M. Dorin,†,‡ Haorong Wang,†,‡ Yan Qiu,†,‡ Eric N. Coker,† William A. Steen,† James E. Miller,† and John A. Shelnutt*,†,§

Advanced Materials Laboratory, Sandia National Laboratories, Albuquerque, New Mexico 87106, Department of Chemical and Nuclear Engineering, University of New Mexico, Albuquerque, New Mexico 87131, and Department of Chemistry, University of Georgia, Athens, Georgia

Received August 3, 2007; Revised Manuscript Received October 23, 2007

ABSTRACT

Platinum nanowire networks have been synthesized by chemical reduction of a platinum complex using sodium borohydride in the presence of a soft template formed by cetyltrimethylammonium bromide in a two-phase water-chloroform system. The interconnected polycrystalline nanowires possess the highest surface area (53 ± 1 m^2/g) and electroactive surface area (32.4 ± 3.6 m^2/g) reported for unsupported platinum nanomaterials; the high surface area results from the small average diameter of the nanowires (2.2 nm) and the 2–10 nm pores determined by nitrogen adsorption measurements. Synthetic control over the network was achieved simply by varying the stirring rate and reagent concentrations, in some cases leading to other types of nanostructures including wormlike platinum nanoparticles. Similarly, substitution of a palladium complex for platinum gives palladium nanowire networks. A mechanism of formation of the metal nanowire networks is proposed based on confined metal growth within a soft template consisting of a network of swollen inverse wormlike micelles.

Nanostructured platinum is important in many technical applications, including as an electrocatalyst in proton exchange membrane fuel cells[1,2] and as catalysts in many reactions including solar water-splitting devices.[3,4] However, the high cost and limited supply of platinum in these applications remain a challenge that demands its efficient commercial usage. The manipulation of the size and shape of platinum materials at the nanoscale can contribute to lowering Pt usage and achieving the necessary cost reduction.[5−8] Previous efforts to produce platinum in various shapes have produced Pt nanowires,[9,10] tetrahedra, and octahedra[11] using the polyol method. Cubic, cuboctahedral, and porous Pt nanoparticles have been synthesized using a capping polymer combined with differing reduction conditions.[12−14] Pt nanotubes[15] and mesoporous Pt films[16,17] were obtained by chemical and electrochemical reduction of Pt salts confined within the aqueous environment of the lyotropic liquid crystalline phases of surfactants. In addition, Pt multipods have been synthesized by an induced anisotropic growth in organic solvents,[18] and very recently monodispersed Pt nanocubes have been obtained by decomposing a Pt precursor with pressurized hydrogen.[19] Finally, using templating assemblies such as peptide tubes, surfactant micelles, multilamellar vesicles, unilamellar liposomes, and liposomal aggregates, with/without incorporated molecular photocatalysts, our group has successfully synthesized a series of platinum nanostructures with shape control, which include peptide-nanotube/nanoparticle composites,[20] globular nanodendrites,[21,22] flat dendritic nanosheets,[22,23] foamlike nanospheres composed of convoluted dendritic sheets,[22,23] and porous nanocages.[24]

Herein, we report the synthesis of platinum nanowire networks based on a modified phase-transfer method, similar to that originally developed by Brust et al. in the 1990s.[25−27] Our approach is simple, environmentally friendly, and can be scaled up readily. Shape selectivity in this case relies on the formation of a network of wormlike micelles within an organic solvent phase that acts as a soft template for metal growth. On the basis of a templateless method, Ramanath and his co-workers[28,29] have prepared Ag and Au nanowire networks via assembly of nanoparticles at water/toluene interface. However, this templateless strategy has not been shown to be capable of producing metallic nanowire networks other than Ag and Au. Using hard templates like the interconnected channels of mesoporous silica, similar platinum nanowire networks have been prepared by chemical[30] and electrochemical deposition[31,32] of platinum followed by the removal of the silica framework. However, these methods generally produce poor networks because of the

* Corresponding author. E-mail: (Y.S.) ysong@sandia.gov; (J.A.S.) jasheln@unm.edu.
† Sandia National Laboratories.
‡ University of New Mexico.
§ University of Georgia.

10.1021/nl0719123 CCC: $37.00
Published on Web 11/14/2007

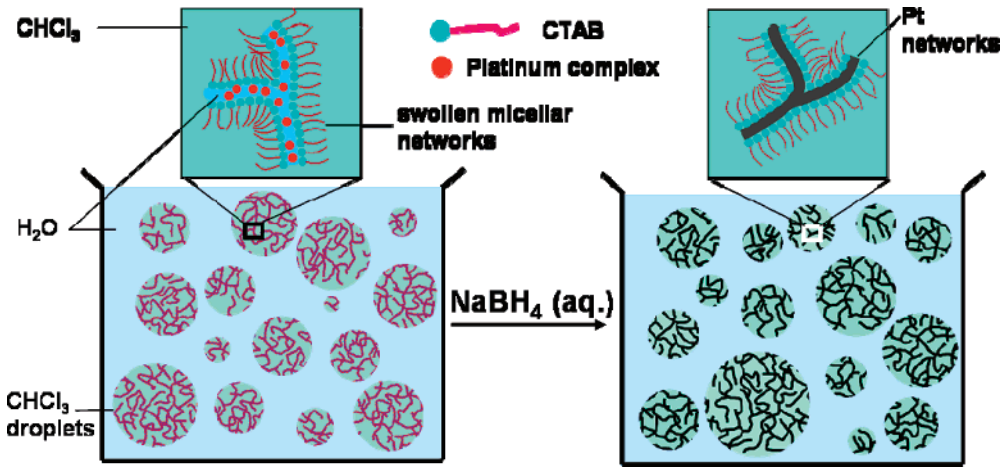

Figure 1. Illustration of the putative soft template with the wormlike micellar network formed inside droplets of chloroform on the left and the developed platinum nanowire networks formed by reduction of Pt complex within the template on the right. The emulsion system aids in providing mass transport of Pt complex and reductant into the wormlike micelles.

difficulty of making and completely filling high-quality mesoporous silica templates to ensure interconnectivity. In addition, the use of hydrofluoric acid to remove the silica template poses environmental and safety concerns for this earlier approach. Limited control over the size and structure of the networks is possible when using hard inorganic templates.

In the approach taken here, a soft surfactant template is used to produce extended well-formed platinum nanowire networks. In a typical synthesis, 10 mL of a 20 mM K_2PtCl_4 aqueous solution, aged for at least a day, was mixed with 10 mL of chloroform containing 40 mM cetyltrimethylammonium bromide (CTAB) while stirring. This two-phase aqueous and chloroform mixture with added CTAB was chosen because previous studies have suggested that wormlike micelles, which may also form interconnected networks, are likely formed under these conditions. Specifically, Evans et al.[33]and Smith and co-workers[34] showed that bicontinuous micellar structures formed in a region of the ternary phase diagram of didodecyldimethylammonium bromide (DDAB)/water/alkane system, a system similar to the CTAB/water/chloroform system used to form wormlike micelles in the present work. Another study by Moulik et al.[35] gave the approximate phase diagram for the CTAB/water/chloroform system. Although the study did not provide a detailed structural analysis of the phase region used for our nanowire preparations, they described it as a "gel", which is consistent with our observation of turbidity and a tubular micellar network. Evidence for network formation is provided by a method suggested by Evans et al.[36] for determining the extent of continuity of the water channels in the swollen wormlike micellar network. If the conductivity (or resistance) is measured for separated inverse micelles, the resistance is high because the water content is encapsulated and surrounded by the continuous oil phase. In contrast, for a bicontinuous structure such as the putative micellar network, the resistance is substantially lowered because the more conductive water channels provide an interconnected water path through the liquid. Indeed, the resistance measured for the 2 mM CTAB/water/chloroform micellar system, which is not expected to form an interconnected micellar network (probably spherical micelles), was infinite (out of measurement range) while the resistance of the putative wormlike inverse micellar network composed of 40 mM CTAB/water/chloroform was determined to 3.0 MΩ. Thus, the resistance of the presumed micellar network is close to that of pure water (2.2 MΩ), whereas the resistance of the putative spherical micellar system is much higher.

The proposed reaction system is illustrated in Figure 1. Initially, the swollen wormlike micelle networks (bicontinuous conduits) are formed within the chloroform droplets with the CTAB molecules residing at the interface between the chloroform phase and the water pools containing the Pt complex inside the micelles. The Pt complex, confined within the inverse micellar network, is then reduced under the reaction conditions described below to give Pt nanowires that replicate the structure of the micellar network template.

To transfer the Pt complex into the chloroform phase, the mixed chloroform and water phases prepared as described above were stirred, and to achieve complete transfer the CTAB concentration needed to be twice that of the Pt complex. After at least 10 min, stirring was discontinued allowing the water and chloroform phases to separate from each other over a period of 2 h. Figure 2 (inset) shows that phase transfer of the orange Pt(II) complex to the micelle-containing chloroform phase at the bottom of the bottle is complete, leaving the aqueous phase (top) colorless and transparent. Complete transfer is confirmed by the UV−visible spectrum in Figure 2. Before stirring, characteristic absorption peaks of the platinum complex were observed in the aqueous phase (black line), but after stirring the three peaks disappeared (green line) while new peaks appeared in the chloroform phase (red). The unique hydrophobic/hydrophilic environment at the water/CTAB/chloroform interface of the wormlike micelles (shown in the expanded views in Figure 1) must drive the transfer between phases, and the electrostatic interaction between the positively charged CTAB molecules and the negatively charged platinum complex likely plays an important role in facilitating the transfer.

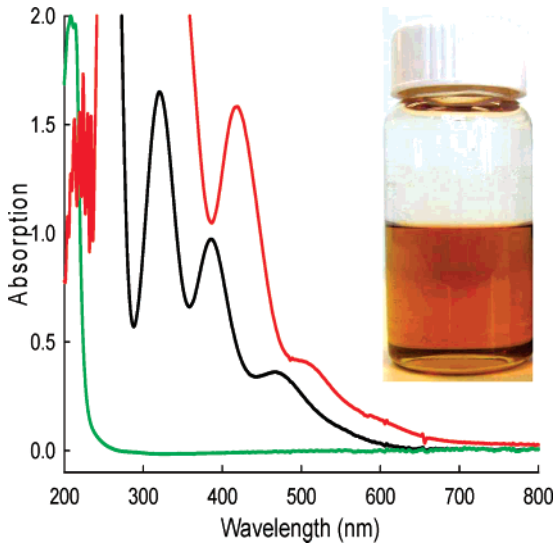

Figure 2. UV−vis spectrum of aqueous 20 mM K_2PtCl_4 before (black line) and after phase transfer (green line) and the chloroform phase after phase transfer (red line). Inset: a photograph of the separated water (top) and chloroform (bottom) phases after transfer of the platinum complex.

For Pt(II) reduction, this mixture was then transferred to a 125 mL glass bottle, and 80 mL of Nanopure water and 10 mL of 300 mM sodium borohydride was added while stirring at a speed of 1000 rpm. The mixture turned black immediately accompanied by bubbling, indicating the reduction of Pt complex to nanoscale platinum metal, and samples were prepared for electron microscopy.

Transmission electron microscopy (TEM) images reveal the presence of abundant platinum nanowires in a low-magnification image (Figure 3a). The nanowires have an average cross-sectional diameter of 2.2 ± 0.3 nm as determined by manually measuring 100 randomly selected sections of the wires (see Figure S1). The nanowires have uniform diameters with the ratio of the standard deviation to the average diameter of 13.6%. At higher magnification (Figure 3b), the nanowires are seen to interconnect to form large extended wire networks. High-resolution TEM (HR-TEM) images (Figure 3c) show that the interconnected nanowires are polycrystalline as revealed by the varied orientations of the atomic lattice fringes along an individual continuous wire. Scanning electron microscopy (SEM) images were also obtained. The SEM images in particular, such as the one in Figure 3d, show particularly well how the nanowire network forms a three-dimensional porous mass and also verifies that the diameters of the platinum nanowires are uniform.

The X-ray diffraction pattern of the Pt nanowire network is as expected for randomly oriented face-centered cubic Pt crystals (Figure 4). In particular, the peaks attributed to the 111, 200, and 220 reflections exhibit broadenings consistent with the nanoscale structural features seen by electron microscopy.

High surface area is anticipated for nanowire networks with diameters as small as 2.2 nm. The surface area of the Pt network material was measured after successfully scaling

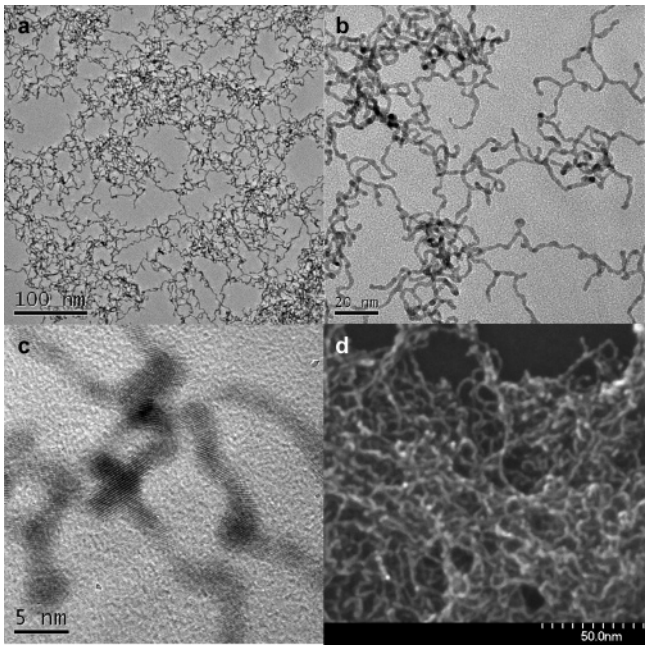

Figure 3. TEM images (a,b), HRTEM image (c), and SEM image (d) of the platinum nanowire network. Reaction conditions: 20 mM Pt(II) and 40 mM CTAB in 10 mL of chloroform; 30 mM $NaBH_4$ in 100 mL of water; stirring at 1000 rpm.

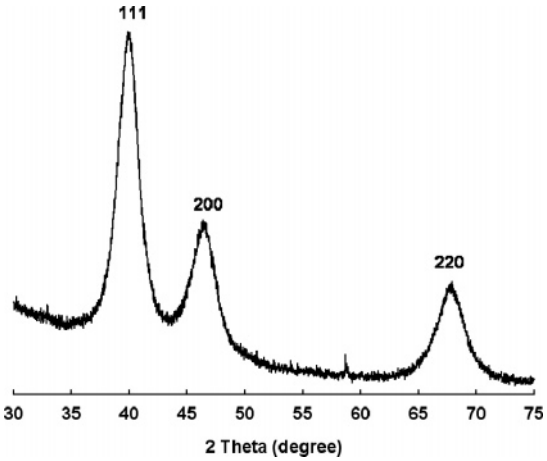

Figure 4. X-ray diffraction pattern of the platinum nanowire network.

up the synthetic protocol to provide the quantity necessary for the N_2 adsorption analysis. Analysis of isotherms of the nanowire networks like that shown in Figure 5 gives a surface area of 53 ± 1 m^2/g, which is to our knowledge the highest area reported for unsupported Pt materials. The Barrett−Joyner−Halenda (BJH) pore-size analysis[37] gives a distribution of pore sizes ranging from 2 to 10 nm (Figure 5, inset), but the broadness of the distribution indicates that the pores are not well defined. These pores most likely correspond to the void space of the densely packed platinum nanowire networks observed in the TEM and SEM images (Figure 3). Other than the hollow Pt nanocages[24] and the globular nanodendrites[21] previously reported by us, we are aware of only one other example of a nanoporous Pt material (prepared by electrochemical reduction of platinum salts confined in the aqueous environment of liquid crystalline phase), and

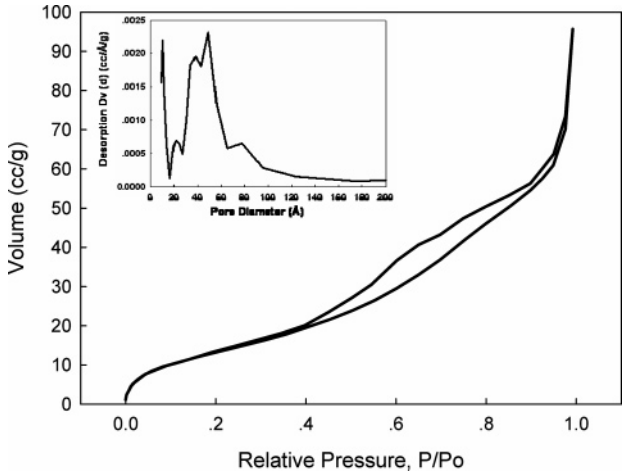

Figure 5. N_2 adsorption/desorption isotherm of the platinum nanowire networks. Inset: BJH pore-size distribution curve obtained from the desorption data.

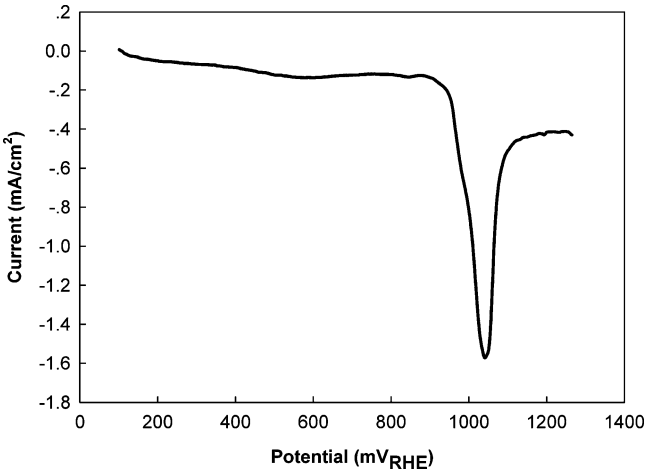

Figure 6. A representative CO-stripping voltammogram for the platinum nanowire networks.

this material has a surface area of 22 ± 2 m^2/g.[16,17] High active surface area is desirable for catalytic and electrocatalytic applications such as fuel cells. The electroactive surface area determined from CO-stripping voltammograms like that shown in Figure 6 is found to be 32.4 ± 3.6 m^2/g (see experimental details in the Supporting Information). This active surface area is the highest of all unsupported platinum materials.

Interestingly, the size of the network intersections and the diameter of the Pt nanowire can be tuned somewhat by simply varying the stirring rate and the concentration of Pt salt, respectively. By variation of the stirring rate from 0 to 1000 rpm, the Pt nanostructures evolved as shown in the TEM images of Figure 7. At 0 rpm, the product contains only a few nanowires growing out from many 5−10 nm irregular particles and possibly bridging between them. At the 200 rpm stirring rate, more nanowires and fewer and smaller nanoparticles (mostly smaller than 5 nm) are produced. At this stage, it is clear that the knoblike particles are all integrated into the platinum nanowire networks. For 700 rpm stirring, the nanowire network dominates the Pt nanomaterial, but 4 nm knobs still form at some of the

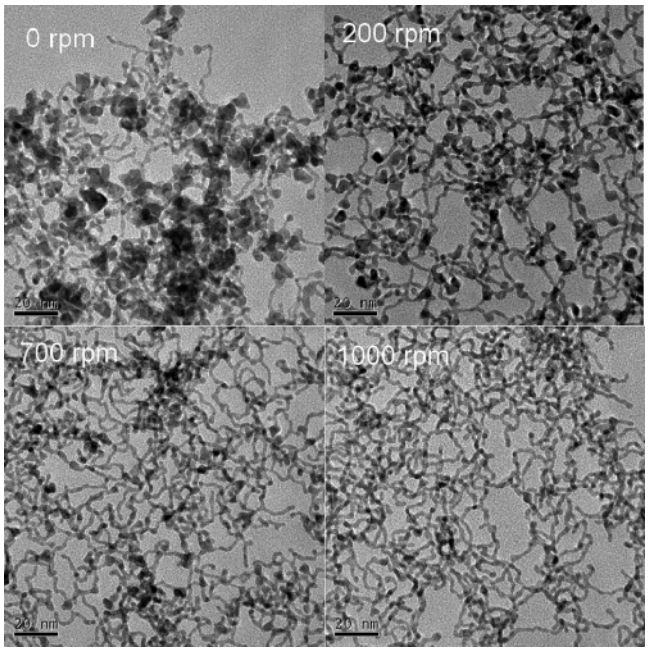

Figure 7. TEM images of the platinum nanostructures obtained with stirring rates of 0, 200, 700, and 1000 rpm. Other reaction conditions: 20 mM Pt(II) and 40 mM CTAB in 10 mL of chloroform mixed with 30 mM $NaBH_4$ in 100 mL of water.

intersecting points and at the ends. At 1000 rpm, the largest quantity of Pt nanowire networks is produced without clear evidence of enlargements at the intersections of the network. At the highest stirring rate of 1300 rpm, the structural features of the networks are the same as those synthesized using 1000 rpm (image not shown). This series of experiments demonstrates the importance of mass transfer of borohydride across the water/chloroform interface in the synthesis. At stirring rates of 1000 rpm and larger, large numbers of small chloroform droplets are created providing increased surface area to allow more efficient diffusion of borohydride into the micelles and correspondingly increased rates of reduction of Pt complex throughout the surfactant micellar network. Thus, rapid reduction presumably captures a snapshot of the templating micellar network structure in the form of the Pt metal network with no significant structural evolution of the soft template. In contrast, at slow stirring speeds, knoblike particles form at the intersections. These are likely the initial nucleation sites from which metal growth occurs. However, because of the slower mass transfer rate, the growth rate is slow enough to allow the micellar template to adjust to the growth resulting in the knob-like particles.

The platinum salt concentration controls the diameter of the nanowires in the network, albeit over a narrow range. For example, when 10 mL of 1 mM K_2PtCl_4 was used with a stirring rate of 1000 rpm, the platinum nanowire network shown in Figure 8a was obtained. For comparison, Figure 8b shows the nanowire network obtained when prepared in the same way except with 20 times the platinum salt concentration (20 mM K_2PtCl_4). In the former case, the nanowires of the network possess a smaller average diameter (1.8 ± 0.3 versus 2.2 ± 0.3 nm), as determined by manually measuring 100 different sections of the network (Supporting

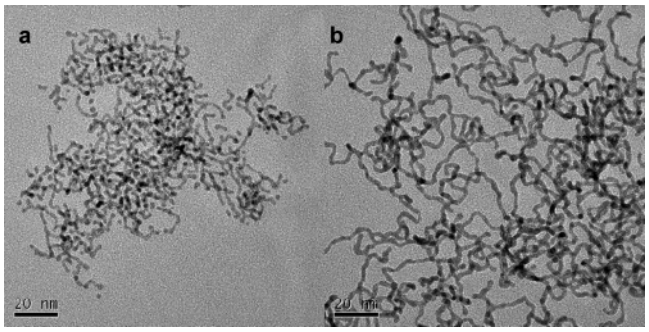

Figure 8. TEM images of the platinum nanostructures obtained using 1 mM (a) and 20 mM (b) platinum complexes in 10 mL of chloroform containing 40 mM CTAB. Other reaction conditions: 30 mM $NaBH_4$ in 100 mL of water; stirring at 1000 rpm.

Information, Figure S2). The reduced size obtained at the low Pt(II) concentration might be expected due to the reduced source of metal ions for reduction in the wormlike micelles. A few separate particles are also observed in Figure 8a further suggesting that there may not be enough platinum available to link up all the wires.

The Pt nanowire networks obtained are consistent with the anticipated structure of the templating surfactant micellar network. Furthermore, additional metal-reduction experiments support the view that the platinum network structure faithfully reflects the structure of the templating micellar network. First, if the soft template controls the metal network structure then other metals besides Pt should give similar nanowire networks. In this regard, when K_2PtCl_4 is replaced in the synthesis by K_2PdCl_4, palladium nanowire networks do form as expected (Supporting Information, Figure S3). Although the structure of the Pd nanowire network is significantly different, the small morphological differences in the Pt and Pd networks may result from differences in the template structure due to differing interactions of the Pt and Pd complexes with micellar interface or perhaps from differing growth habits of the two metals. Second, the spherical micelles, expected at a low concentration of CTAB (2 mM) instead of the wormlike micelles at high CTAB concentration (40 mM), should result in a change in the morphology of the metal. Indeed, small spherical and branched cylindrical Pt nanoparticles were produced (Supporting Information, Figure S4) instead of the Pt nanowire networks (Figure 8a). Thus, the interconnected wormlike micellar networks and separate spherical micelles that are likely present in these two reaction systems lead to different Pt morphologies as expected. Third, when CTAB is left out of our reaction system and the platinum complex stays in the aqueous phase, no Pt nanowire networks should be obtained due to the absence of the soft template. Indeed, without CTAB the reaction gives black precipitate at the water/chloroform interface, indicating reduction of the complex. Figure S5 of Supporting Information shows that the black precipitate is composed of aggregated platinum nanoparticles instead of Pt networks. This experiment demonstrates that the presence of soft CTAB templates is crucial for the preparation of the platinum nanowire network, consistent with the suggested formation mechanism.

In conclusion, polycrystalline platinum nanowire networks with uniform wire diameters were synthesized by using a network of wormlike micelles as a soft template for metal growth. Pileni[38] has recently reviewed the role of soft templates in controlling the size and shape of nanomaterials, especially emphasizing the potential of soft templates for shape control. As an example, he discussed the possibility of using swollen interconnected micelles as a soft template for synthesizing copper nanorods,[38] but a metal network was not produced. This study provides a clear demonstration of the use of soft micellar networks as templates for the successful synthesis of interconnecting metal nanowires that accurately reflect the micellar network structure. The structural features of these platinum networks can be controlled to some degree, including the diameter of the wires and the size of knobs formed at intersecting points. A possible formation mechanism (Figure 1) based on soft templating by the micellar networks contained in chloroform droplets is proposed. The platinum nanowire network has the highest surface area and electroactive surface area reported for unsupported platinum nanomaterials and therefore is expected to have potential applications in catalysis and electrocatalysis. This work opens new opportunities for employing other soft templates to realize shape control over metallic nanomaterials.

Acknowledgment. This work was partially supported by the Office of Basic Energy of Sciences, U.S. Department of Energy. Sandia is a multiprogram laboratory operated by Sandia Corporation, a Lockheed Martin Company, for the United States Department of Energy's National Nuclear Security Administration under Contract DEAC04-94AL85000.

Supporting Information Available: Experimental details, plots of frequency versus cross-section diameter of the platinum nanowire networks, TEM and SEM image of the Pd nanowire networks, TEM images of the spherical and cylindrical Pt nanoparticles, and TEM images of the aggregated Pt nanoparticles produced in the absence of CTAB. This material is available free of charge via the Internet at http://pubs.acs.org.

References

(1) Antolini, E. *Mater. Chem. Phys.* **2003**, *78*, 563−573.
(2) Rolison, D. R. *Science* **2003**, *299*, 1698−1701.
(3) Cameron, P. J.; Peter, L. M.; Zakeeruddin, S. M.; Gratzel, M. *Coord. Chem. Rev.* **2004**, *248*, 1447−1453.
(4) Fang, X. M.; Ma, T. L.; Guan, G. Q.; Akiyama, M.; Abe, E. *J. Photochem. Photobiol.* **2004**, *164*, 179−182.
(5) Narayanan, R.; El-Sayed, M. A. *J. Phys. Chem. B* **2004**, *108*, 5726−5733.
(6) Narayanan, R.; El-Sayed, M. A. *Nano Lett.* **2004**, *4*, 1343−1348.
(7) Narayanan, R.; El-Sayed, M. A. *J. Am. Chem. Soc.* **2004**, *126*, 7194−7195.
(8) Narayanan, R.; El-Sayed, M. A. *Langmuir* **2005**, *21*, 2027−2033.
(9) Chen, J. Y.; Herricks, T.; Geissler, M.; Xia, Y. N. *J. Am. Chem. Soc.* **2004**, *126*, 10854−10855.
(10) Chen, J. Y.; Herricks, T.; Xia, Y. N. *Angew. Chem., Int. Ed.* **2005**, *44*, 2589−2592.
(11) Herricks, T.; Chen, J. Y.; Xia, Y. N. *Nano Lett.* **2004**, *4*, 2367−2371.
(12) Ahmadi, T. S.; Wang, Z. L.; Green, T. C.; Henglein, A.; El-Sayed, M. A. *Science* **1996**, *272*, 1924−1926.
(13) Ahmadi, T. S.; Wang, Z. L.; Henglein, A.; El-Sayed, M. A. *Chem. Mater.* **1996**, *8*, 1161−1163.

(14) Lee, H.; Habas, S. E.; Kweskin, S.; Butcher, D.; Somorjai, G. A.; Yang, P. D. *Angew. Chem., Int. Ed.* **2006**, *45*, 7824−7828.
(15) Kijima, T.; Yoshimura, T.; Uota, M.; Ikeda, T.; Fujikawa, D.; Mouri, S.; Uoyama, S. *Angew. Chem., Int. Ed.* **2004**, *43*, 228−232.
(16) Attard, G. S.; Bartlett, P. N.; Coleman, N. R. B.; Elliott, J. M.; Owen, J. R.; Wang, J. H. *Science* **1997**, *278*, 838−840.
(17) Attard, G. S.; Goltner, C. G.; Corker, J. M.; Henke, S.; Templer, R. H. *Angew. Chem., Int. Ed. Engl.* **1997**, *36*, 1315−1317.
(18) Teng, X. W.; Yang, H. *Nano Lett.* **2005**, *5*, 885−891.
(19) Ren, J. T.; Tilley, R. D. *J. Am. Chem. Soc.* **2007**, *129*, 3287−3291.
(20) Song, Y. J.; Challa, S. R.; Medforth, C. J.; Qiu, Y.; Watt, R. K.; Pena, D.; Miller, J. E.; van Swol, F.; Shelnutt, J. A. *Chem. Comm.* **2004**, 1044−1045.
(21) Song, Y. J.; Jiang, Y. B.; Wang, H. R.; Pena, D. A.; Qiu, Y.; Miller, J. E.; Shelnutt, J. A. *Nanotechnology* **2006**, *17*, 1300−1308.
(22) Song, Y. J.; Yang, Y.; Medforth, C. J.; Pereira, E.; Singh, A. K.; Xu, H. F.; Jiang, Y. B.; Brinker, C. J.; van Swol, F.; Shelnutt, J. A. *J. Am. Chem. Soc.* **2004**, *126*, 635−645.
(23) Song, Y. J.; Steen, W. A.; Pena, D.; Jiang, Y. B.; Medforth, C. J.; Huo, Q. S.; Pincus, J. L.; Qiu, Y.; Sasaki, D. Y.; Miller, J. E.; Shelnuttt, J. A. *Chem. Mater.* **2006**, *18*, 2335−2346.
(24) Song, Y. J.; Garcia, R. M.; Dorin, R. M.; Wang, H. R.; Qiu, Y.; Shelnutt, J. A. *Angew. Chem., Int. Ed.* **2006**, *45*, 8126−8130.
(25) Brust, M.; Bethell, D.; Kiely, C. J.; Schiffrin, D. J. *Langmuir* **1998**, *14*, 5425−5429.
(26) Brust, M.; Bethell, D.; Schiffrin, D. J.; Kiely, C. J. *Adv. Mater.* **1995**, *7*, 795.
(27) Brust, M.; Walker, M.; Bethell, D.; Schiffrin, D. J.; Whyman, R. *J. Chem Soc., Chem. Comm.* **1994**, 801−802.
(28) Maddanimath, T.; Kumar, A.; D'Arcy-Gall, J.; Ganesan, P. G.; Vijayamohanan, K.; Ramanath, G. *Chem. Comm.* **2005**, 1435−1437.
(29) Ramanath, G.; D'Arcy-Gall, J.; Maddanimath, T.; Ellis, A. V.; Ganesan, P. G.; Goswami, R.; Kumar, A.; Vijayamohanan, K. *Langmuir* **2004**, *20*, 5583−5587.
(30) Shin, H. J.; Ryoo, R.; Liu, Z.; Terasaki, O. *J. Am. Chem. Soc.* **2001**, *123*, 1246−1247.
(31) Wang, D. H.; Kou, R.; Gil, M. P.; Jakobson, H. P.; Tang, J.; Yu, D. H.; Lu, Y. F. *J. Nanosci. Nanotech.* **2005**, *5*, 1904−1909.
(32) Wang, D. H.; Luo, H. M.; Kou, R.; Gil, M. P.; Xiao, S. G.; Golub, V. O.; Yang, Z. Z.; Brinker, C. J.; Lu, Y. F. *Angew. Chem., Int. Ed.* **2004**, *43*, 6169−6173.
(33) Evans, D. F.; Mitchell, D. J.; Ninham, B. W. *J. Phys. Chem.* **1986**, *90*, 2817−2825.
(34) Tingey, J. M.; Fulton, J. L.; Matson, D. W.; Smith, R. D. *J. Phys. Chem.* **1991**, *95*, 1445−1448.
(35) Mukherjee, K.; Mukherjee, D. C.; Moulik, S. P. *J. Colloid Interface Sci.* **1997**, *187*, 327−333.
(36) Warr, G. G.; Sen, R.; Evans, D. F.; Trend, J. E. *J. Phys. Chem.* **1988**, *92*, 774−783.
(37) Pierce, C. J. *J. Phys. Chem.* **1953**, *57*, 149−152.
(38) Pileni, M. P. *Nat. Mater.* **2003**, *2*, 145−150.

NL0719123